Role of Raman spectroscopy in high pressure research

A. Jayaraman and S. K. Sharma

University of Hawaii at Manoa, Hawaii Institute of Geophysics and Planetology, 2525 Correa Road, Honolulu, Hawaii 96822, USA

Applications of Raman spectroscopy in high pressure research are reviewed. A brief introduction to the techniques is followed by discussion of current work on the following topics: pressure-induced amorphization, crystal to crystal phase transitions in some molybdate and tungstate compounds, phase transitions in copper metagermanates, and the high pressure behaviour of solid hydrogen and deuterium.

THE advent of the diamond anvil cell in high pressure research opened the window for Raman scattering studies to probe the high pressure behaviour of materials. In the past two decades, several refinements introduced in laser Raman techniques, such as micro Raman, CCD detectors, and confocal optics, have made it possible to obtain Raman signals up to megabar pressures from extremely small sample volume, dictated by the size of the pressure chamber in the diamond cell. One of us reviewed the advances in the field in 1989 (ref. 1) with some illustrative examples; here we review the current status in the field, as a tribute to the great scientist whose explorations with light seven decades ago opened the door to vistas unimaginable then.

Earlier laser Raman studies in the diamond cell were carried out with the fine focusing optics. The current trend is to use a micro-Raman setup such as the one shown in Figure 1 (ref. 2). With the optical arrangement shown in the insert on top of the figure, the set-up becomes a confocal micro-Raman system, resulting in a significant improvement in the signal-to-background ratio. The laser beam from an Ar^+ or a Kr^+ laser is focused to a beam diameter of ~ 3 μm with a long working distance microscopic objective. Either the ~45° angle excitation with respect to the microscope-diamond cell axis (equivalent to a 135° scattering geometry), or 180° geometry (back scattering) is adopted. The 45° geometry is shown in Figure 1. In the 180° scattering geometry, suitable attachments for vertical illumination are provided and a single objective serves for focusing the laser beam on the sample and collection of scattered radiation. The 45° illumination helps in reducing stray light from entering into the system. The scattered light is imaged through the microscope and focused on the slit of the spectrometer with a high quality, short focal-length lens. The introduction of a holographic filter between the lens and the slit helps to reduce the Rayleigh scattered radiation. A triple spectrograph of the type SPEX 1877 equipped with a liquid nitrogen cooled CCD detector is a most convenient Raman spectrometer system to employ. Typically, the spectra are recorded with entrance slits of the spectrograph set at 50 to 200 μm for a resolution of 5 to 20 cm^{-1}.

Any type of diamond cell can be used with system[3]. The one shown in Figure 1 is the Mao-Bell type diamond cell, with beveling and suitable openings on the cylinder side to facilitate the 45° laser beam entry and exit. The diamond anvils for Raman work have to be low fluorescence type and are usually 1/3 carat in size, with anvil flats varying from 700 μm to 300 μm. For multimegabar pressures, it is the general practice to use beveled anvils. In these anvils, the beveled diameter is typically 300 μm and the central flat 50–30 μm in diameter. The bevel angle is variable but is optimally about ~7°.

For pressure media, a mixture of 4:1 methanol/ethanol is commonly used and this medium is found to be hydrostatic up to 10 GPa. Noble gases (He, Ar, Xe) can be used as pressure media and this is accomplished either by cryogenic filling or by high pressure gas loading techniques[3]. Recent experiments have shown that argon is not a very good hydrostatic pressure medium, as was believed earlier[4]. Argon solidifies near 1.2 GPa at room temperature and turns into a quasihydrostatic medium. Helium is found to be far superior. It solidifies near 12 GPa at room temperature and continues to be a soft solid to much higher pressures, viz. 40 GPa (ref. 5). In recent high pressure X-ray diffraction studies on solid hydrogen up to 120 GPa, helium as a pressure medium has been found to be extremely satisfactory in preserving the integrity of the single crystals[6]. But both argon and xenon are easier to handle and provide a nonreactive and clean background for samples. They can be used, provided the behaviour of the sample is not dependent on the state of the stress exerted by the pressure environment. Helium is much more compressible and lighter and hence somewhat more difficult to trap in the gasket hole of the diamond cell.

The ruby fluorescence technique is commonly used for pressure calibration, for it is quick, sensitive and efficient. However, the ruby peaks progressively become

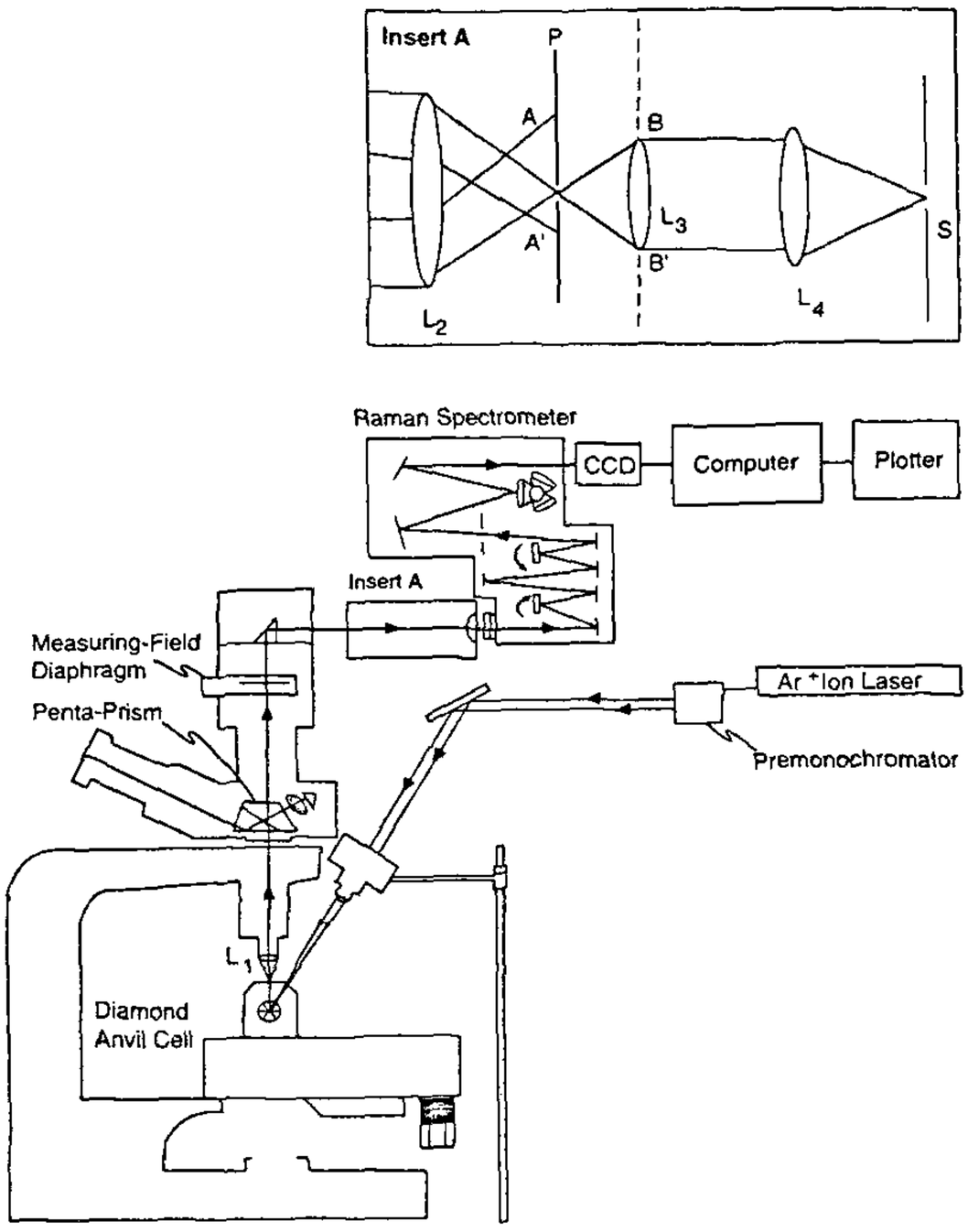

Figure 1. Micro-Raman system. The microscope has a pentaprism to view the sample, a diaphragm and back lighted spectrometer slits. Insert A shows the confocal imaging attachment. The confocal arrangement allows detection of light originating from a small focal volume, with little or no contamination of light scattered from regions away from the focus. This is achieved by placing a pinhole in the image plane.

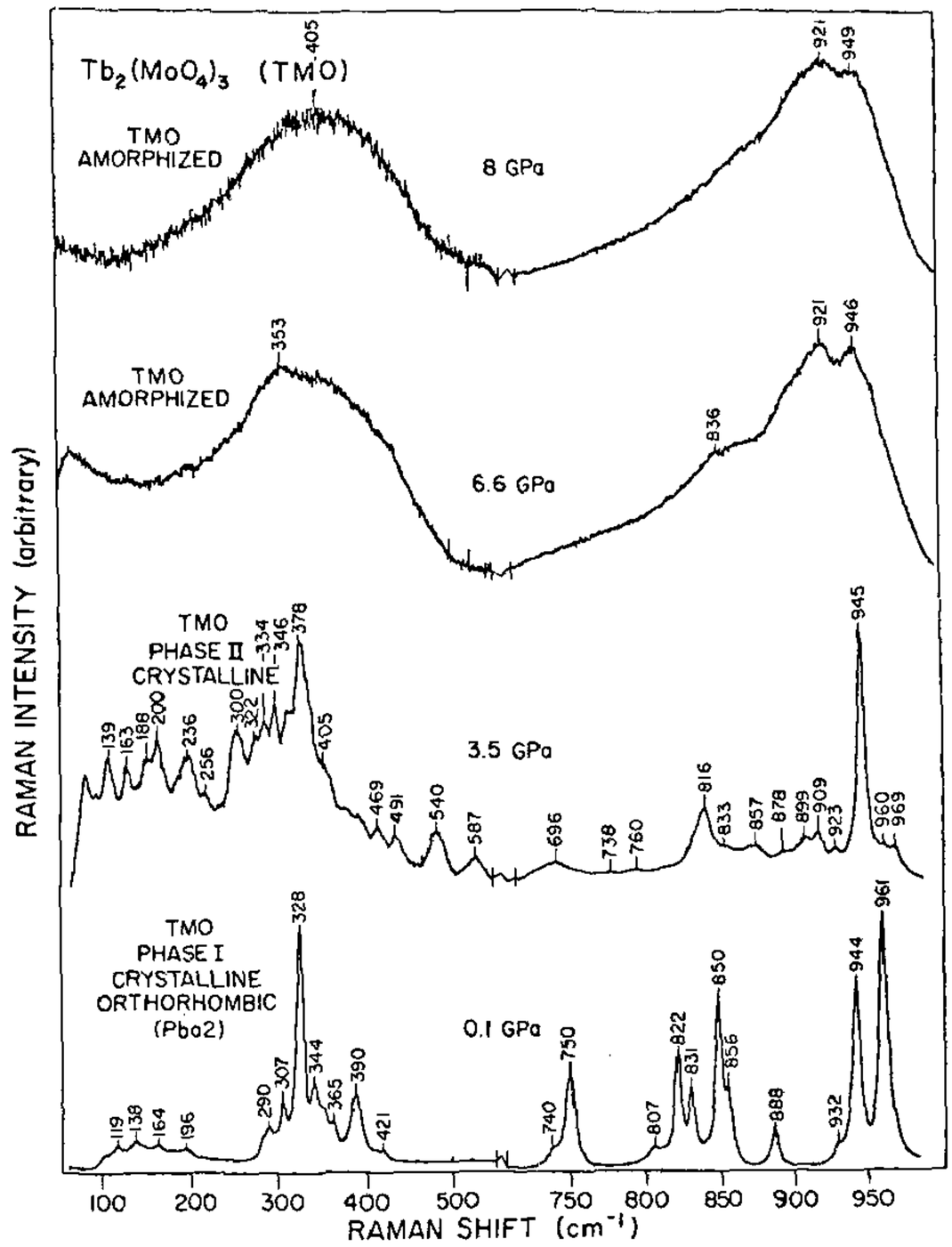

Figure 2. Raman spectra of $Tb_2(MoO_4)_3$ at four different pressures demonstrating pressure-induced amorphization. Note the broad feature in the 6.6 GPa and 8 GPa spectra due to amorphization. A crystal-to-crystal phase transition is also seen in the 3.5 GPa spectrum.

weaker with pressure and also broaden if the pressure medium is nonhydrostatic. Further, diamonds are found to develop pressure-induced fluorescence in the megabar region[7,8] and this interferes with the already weakened ruby emission. Recently, the use of diamond anvils made from synthetic isotopically pure C^{13}-diamond have been suggested to avoid this problem. Diamond anvils of C^{13} are reported to be good up to 300 GPa (ref. 9), as far as pressure-induced fluorescence is concerned. But the cost of these diamonds is prohibitive for general use at present. Excellent Raman spectra can be obtained with low-fluorescence Type I diamonds up to 50 GPa, and most systems of interest to condensed matter physics or materials science fall within this pressure range[1].

Raman spectroscopic studies at high pressure

Some general remarks

Raman spectroscopy is a very convenient tool to probe pressure-induced phase transitions[1,10]. Further, the pressure dependence of the vibrational modes contains information on bonding and crystal chemical properties. Structural phase transitions, phase transitions involving subtle changes in the symmetry of the crystal lattice, and transitions to disordered and amorphous state leave their characteristic signatures in the Raman spectra. Through a detailed analysis of these features, the mechanism involved in the phase transitions and what happens to the structural building blocks can be inferred. One of the most active areas in high pressure research in recent years has been pressure-induced amorphization, and in this field Raman spectroscopic studies have played an important role. Pressure-induced structural transitions in many molybdates and tungstates of varying degree of complexity and pressure-induced phase transitions in $CuGeO_3$ have been the focus of study in our Raman laboratory at the University of Hawaii. Another field in which Raman spectroscopy has played a key role is in following the behaviour of solid hydrogen, compressed to multi-megabar pressures[10]. In this article, we will discuss some select cases to show the role of Raman

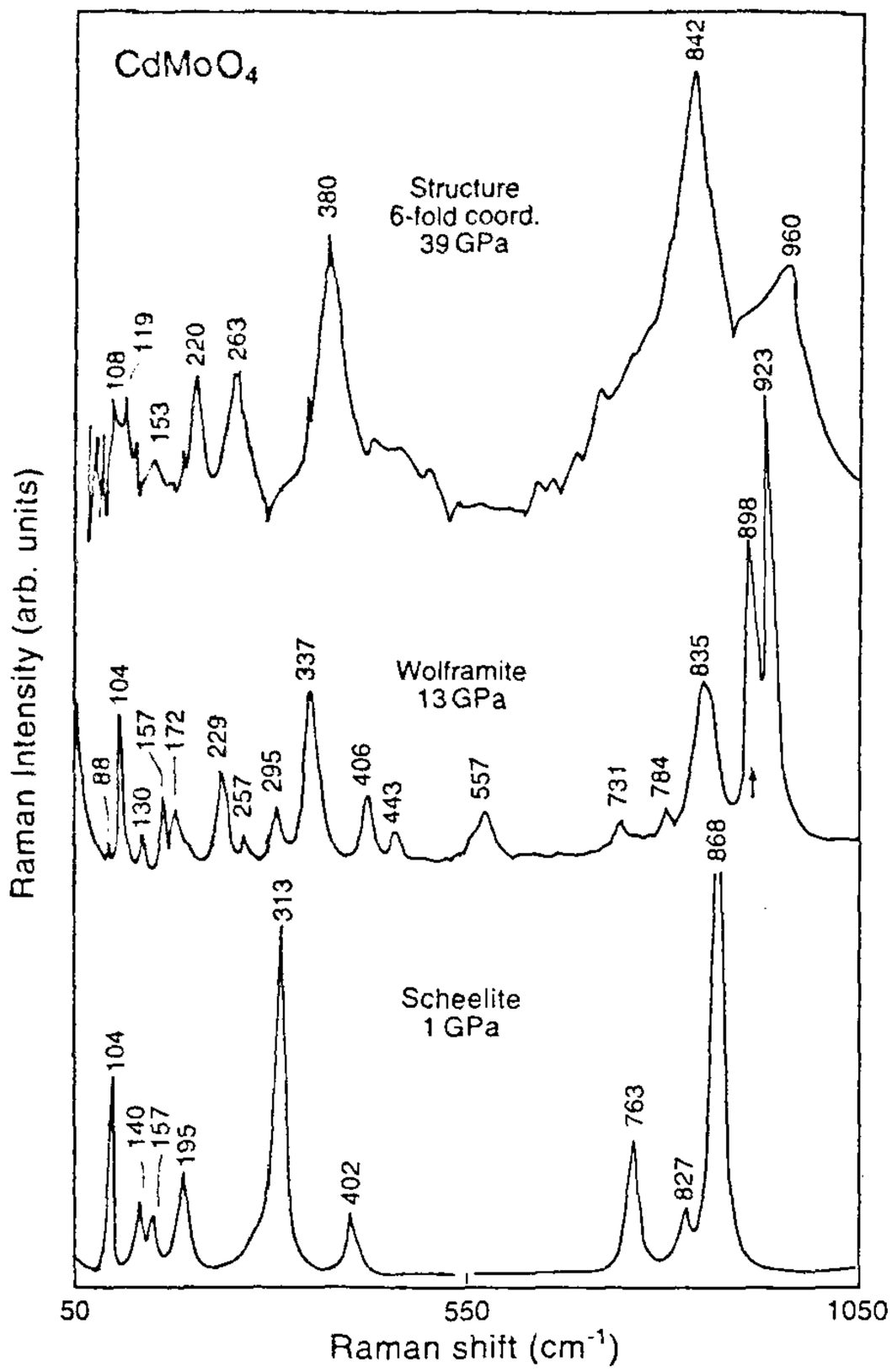

Figure 3. Raman spectra of $CdMoO_4$ at three pressures showing phase transitions from the scheelite structure. The arrow marks the strongest peak of scheelite in the mixed phase spectrum (middle).

spectroscopy in elucidating the high pressure behaviour of materials.

Pressure-induced amorphization

Pressure-induced amorphization has been documented in a number of materials in recent years. Raman spectroscopy has turned out to be one of the convenient and effective probes to establish crystalline to amorphous phase transitions *in situ*. The earliest examples are SnI_4 (ref. 11) and α-quartz[12] and berlenite ($AlPO_4$) (ref. 13). The subject has been reviewed in an excellent article by Sharma and Sikka[14] and in an earlier article in *Current Science* by Sikka[15]. Here we illustrate pressure-induced amorphization, with examples from our Raman studies on some rare earth trimolybdates and dimolybdates.

In Figure 2, *in situ* Raman spectroscopic evidence for pressure-induced amorphization in $Tb_2(MoO_4)_3$ is presented[16]. The sharp Raman features observed in this compound disappear when single crystal or powdered material is compressed at room temperature to pressures above 6 GPa, regardless of whether the compression is carried out in a hydrostatic medium or under quasihydrostatic conditions. The appearance of the two broad Raman features also coincides with the results of *in situ* high pressure X-ray diffraction studies. In amorphization, the sharp X-ray diffraction peaks disappear. On release of pressure, the amorphized phase is metastably retained down to ambient pressure, reverting gradually with time to highly disordered parent-like phase.

The tendency of the rare earth trimolybdate system to amorphize under compression was first reported by Brixner[17] in $Gd_2(MoO_4)_3$. When the β-phase of $Gd_2(MoO_4)_3$ was treated to 6.5 GPa at temperatures $\leq$400°C, Brixner found from X-ray diffraction studies that the quenched material had amorphized. It is now believed that the amorphization in the rare earth trimolybdates is due to the kinetically impeded β -to-α phase transition. The β-phase is metastable low density phase, while the α-phase is the thermodynamically stable, high density phase. Therefore, pressure should drive the β-phase to the α-phase. But at room temperature the system cannot make the structural rearrangements necessary to establish the ordered α-phase structure, and hence in frustration disorders. When heated to temperatures above 700°C near 6 GPa the α-phase is obtained on quenching, indicating that the crystalline to crystalline transition will proceed when the kinetic barrier is removed by temperature activation.

Pressure-induced amorphization near 30 GPa in the dimolybdate system $NaLa(MoO_4)_2$ has been reported[18]. Again the Raman spectra clearly establish that the system disorders. However, in the double molybdates, a much higher pressure is needed to amorphize the system. On release of pressure, the system recovers crystallinity to the parent phase. It is believed that in the double molybdate, the amorphization may be related to a tilting of the (MoO_4) octahedra in an uncorrelated manner. The position of the broad Raman peak at the high frequency end suggests that the individual MoO_4 tetrahedra still survive in the amorphized phase.

Simple molybdates involving divalent cations such as $SrMoO_4$ do not undergo any pressure-induced amorphization up to the highest pressure studied[19]. Thus there seems to be a correlation between structural complexity and pressure-induced amorphization.

In a totally different system, namely copper metagermanate ($CuGeO_3$), we have Raman evidence for pressure-induced amorphization[20]. This system will be discussed elsewhere in this article in more detail.

Pressure-induced structural transitions

$CdMoO_4$ and $CdWO_4$. These two materials crystallize in the scheelite and wolframite structures respec-

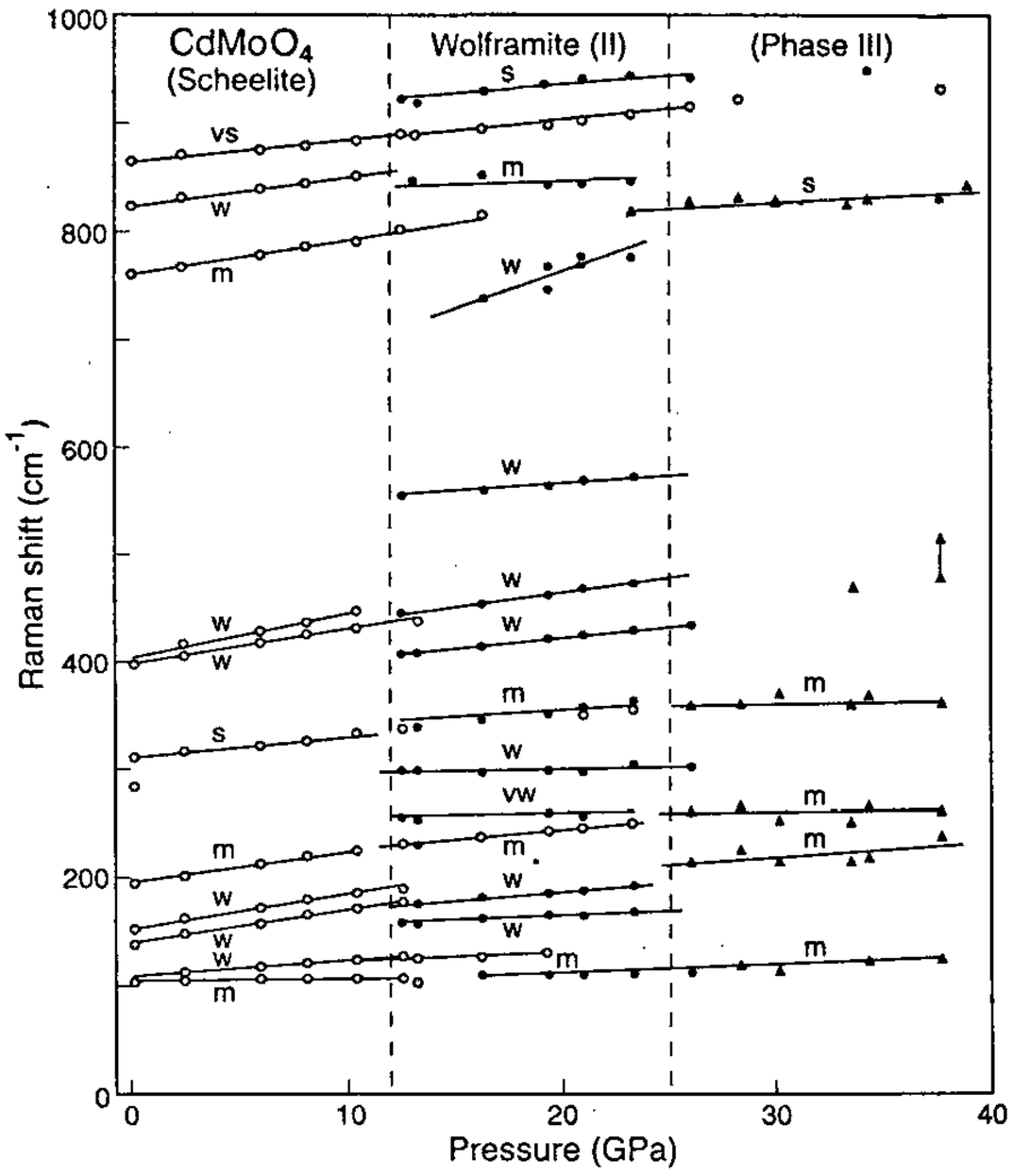

Figure 4. Pressure dependence of the Raman peaks in $CdMO_4$ reflecting the phase transitions. Dotted lines mark the phase transition pressures.

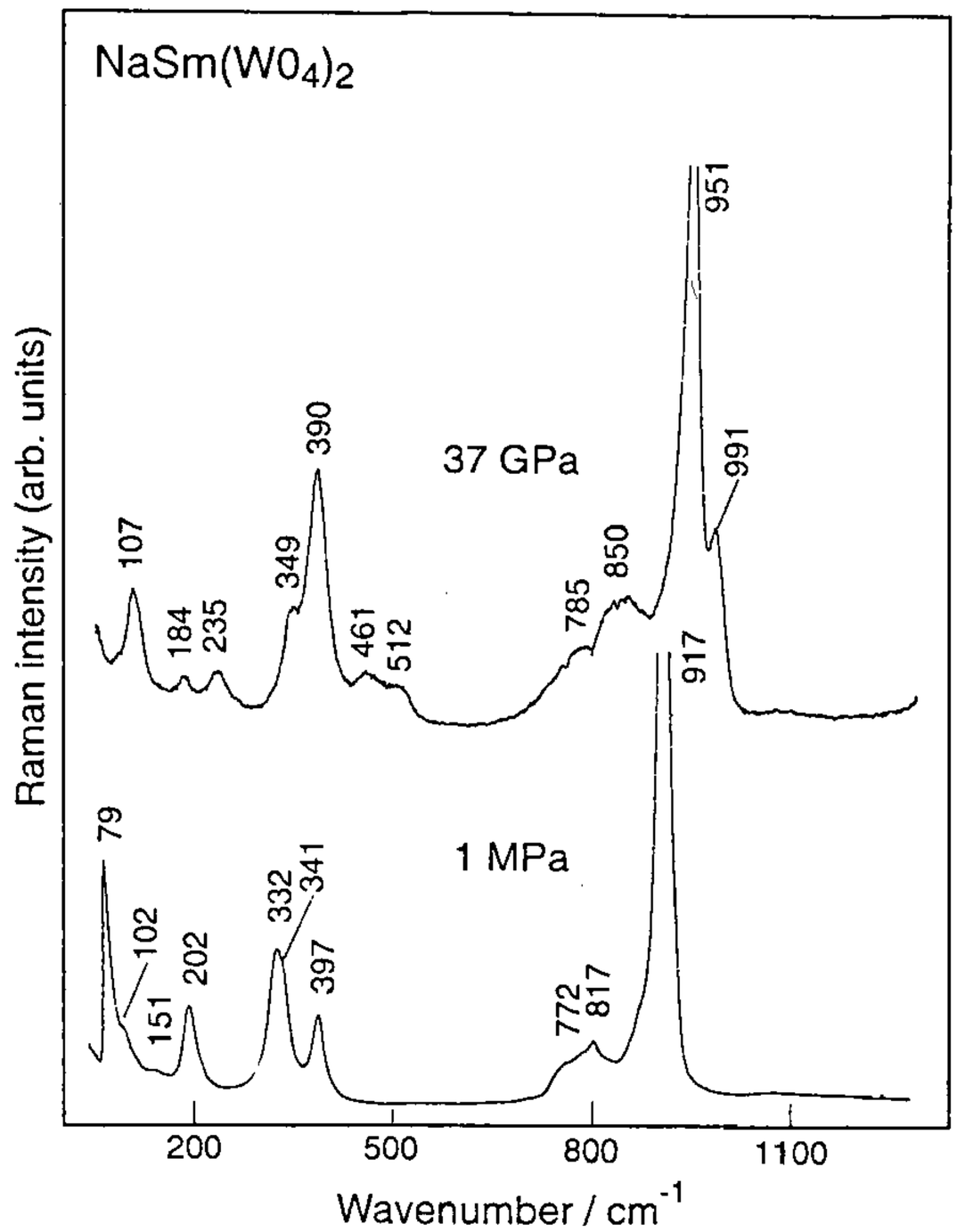

Figure 5. Raman spectra of NaSm $(WO_4)_2$ at two pressures, the scheelite phase at 1 MPa and distorted scheelite at 37 GPa.

tively, typical structures encountered in a large class of ABO_4 type compounds. The Raman spectra of $CdMoO_4$ (ref. 21) in the normal phase and at high pressures are shown in Figure 3. The spectra strikingly change near 13 GPa and near 25 GPa, due to a phase change to the wolframite structure and then to a much denser new structure labelled Phase III. From the shift in the ν_1 Raman peak in Phase III of $CdMoO_4$ (around 840 cm^{-1}), it is inferred that the new structure must involve a change in the coordination of the Mo–O from four-fold to six-fold coordination. The change to higher coordination results in longer Mo–O bond length, which lowers the ν_1 frequency. In $CdWO_4$ (ref. 22), a similar transition occurs near 20 GPa. A convenient way to demonstrate pressure-induced phase transition is by plotting the Raman peak position against pressure, as shown for $CdMoO_4$ in Figure 4. The two phase changes discussed above are clearly seen in the plot.

Alkali–rare earth double molybdates and tungstates. These double molybdates and tungstates crystallize in the scheelite-related orthorhombic or lattice scheelite structure when the cations are disordered. Some of the tungstates have the wolframite structure. A third type has the layered structure typified in the K, Rb, and Cs double molybdate compounds. We have explored the pressure-induced phase transitions in several of them and discuss here a few select cases.

In general, the scheelite type and the closely related orthorhombic (pseudo-scheelite type) materials exhibit a pressure-induced phase transition in the 10–12 GPa region to a distorted version of the above two types, with a lower symmetry[23]. Typically, the high frequency ν_1 Raman peak splits into two peaks and further, some changes occur in the ν_2 and ν_4 mode region. This behaviour is shown in Figures 5 and 6 for $NaSm(WO_4)_2$. At pressures near 30 GPa, they all seem to disorder, as judged from the loss of sharp Raman peaks from the spectrum.

In Figure 7, the pressure-induced phase transition in the layer-type KTb $(MoO_4)_2$ is shown[24]. A first-order phase transition is observed near 3 GPa in which the single crystal plate samples visibly contract in the a-axis direction and change colour to a bright yellow, as seen by transmitted light. The transition involves a change in the crystal structure to a phase with monoclinic symmetry. Identical pressure-induced transitions occur near 3 GPa in KY $(MoO_4)_2$ and KDy $(MoO_4)_2$ (ref. 25) as seen from the Raman features, but there is no change in the colour of the material. This suggests that the colour

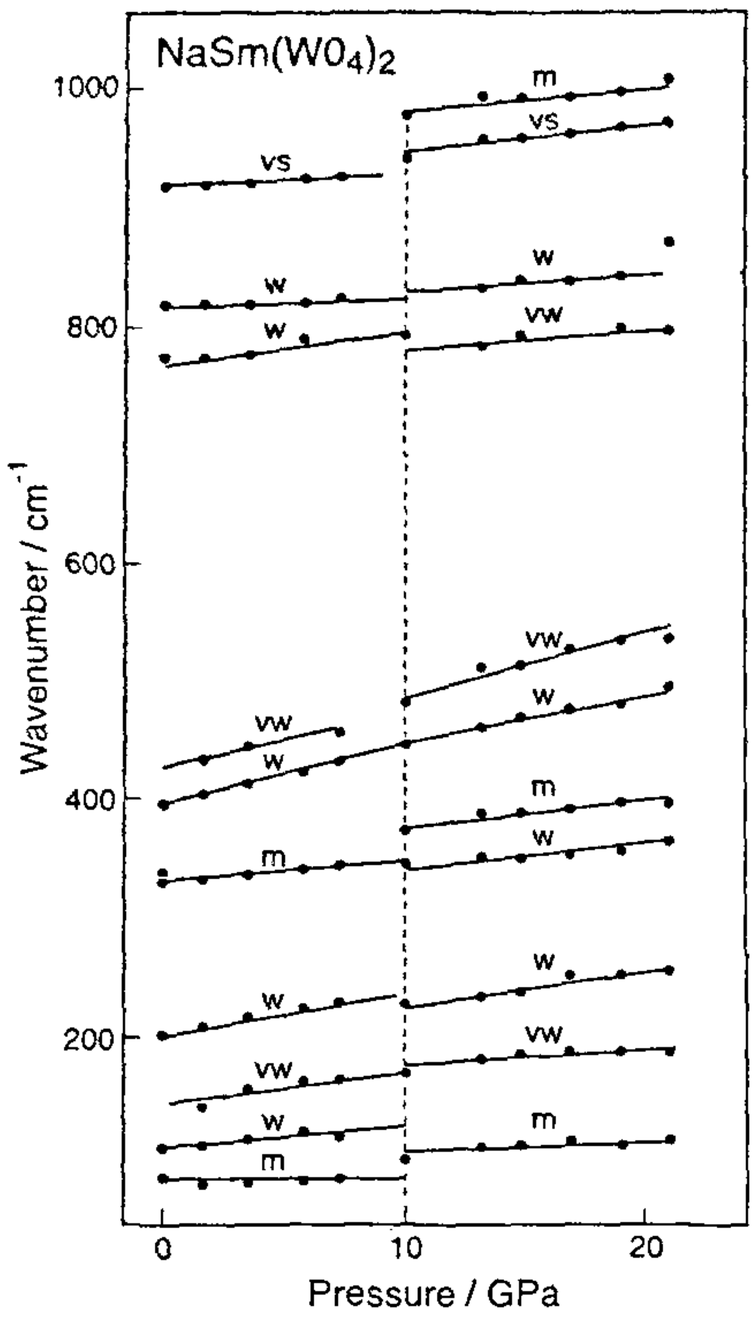

Figure 6. Pressure dependence of the observed Raman peaks in $NaSm(WO_4)_2$. Phase transition marked by the dotted line.

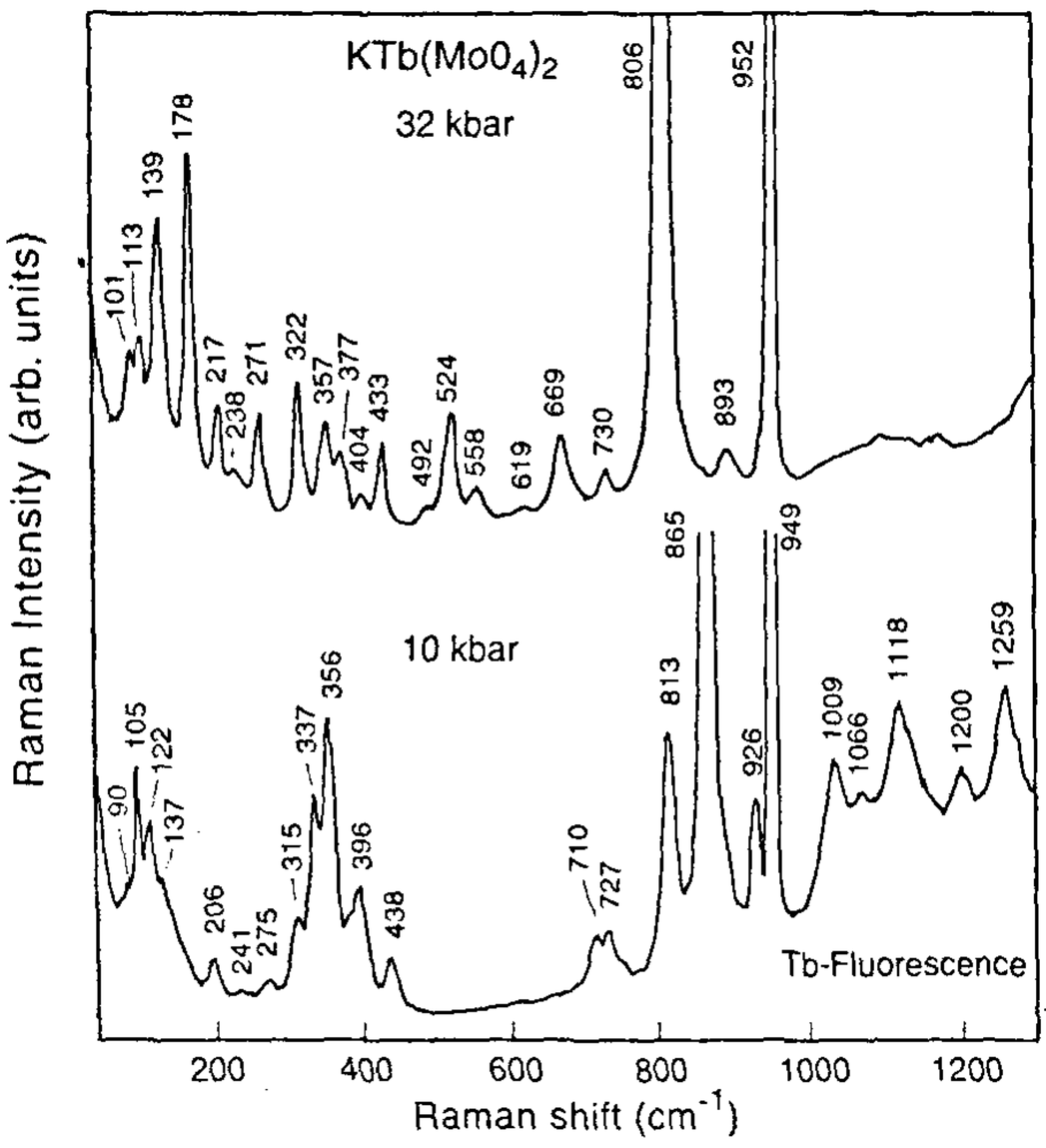

Figure 7. Raman spectra of the normal layer structure type phase and the new high pressure phase of $KTb(MoO_4)_2$.

change observed in $KTb(MoO_4)_3$ must be associated with an electronic transition, and in this connection 4f–5d electron transfer in Tb seems the most likely transition.

The molybdate systems progressively change colour and turn deep orange near 30 GPa. We believe that this is due to a change in the electronic state of Mo, involving a back transfer of charge from the oxygens to Mo^{6+} to compensate for the repulsion of Mo^{6+} experienced by compression of the lattice. The absorption due to this charge transfer (back donation) makes it difficult to obtain Raman spectra above 30 GPa.

$CuGeO_3$. Copper metagermanate is a remarkable material, for it is the only inorganic compound known to exhibit the so-called Spin-Peierls transition at 14 K (ref. 26). The transition is associated with the antiferromagnetic pairing interaction of the Cu^{2+} spins in a Heisenberg-like chain lattice. The material crystallizes in a layered lattice[27] whose structural building blocks consist of chains of corner-linked GeO_4 tetrahedra and CuO_6 edge-sharing octahedra, running parallel to each other. Actually the GeO_4 chains are linked by Cu^{2+} which lie on a chain surrounded by a distorted octahedron of oxygens belonging to four adjacent GeO_4 chains. The structure is related to the pyroxene type silicates such as $MgSiO_3$, with the difference that in the latter the SiO_4 tetrahedra lie on either side of the chain, whereas in $CuGeO_3$ the GeO_4 tetrahedra lie on the same side. In the mineralogical nomenclature this disposition of tetrahedra is known as 'einer' chain, and $CuGeO_3$ is the only compound known to have this unique arrangement[28]. This is attributed to the tendency of the Cu^{2+} to occupy a distorted octahedral site because of the Jahn–Teller effect[29]. The structure can easily be altered by external constraints such as pressure and indeed this occurs. Three structures compete when the system is pressurized, and surprisingly the hydrostaticity of the pressure medium determines the transition sequence. *In situ* high pressure Raman studies have yielded a wealth of information on these pressure-induced phase transitions[30]. The resulting high pressure phases are very colourful because of the changes in the electronic state associated with Cu^{2+}. The results of the Raman spectroscopic characterization of the phases and optical microscopic studies have appeared in the columns of *Current Science*[30]. Here we present a brief description of the behaviour of the system.

Raman spectroscopic studies on single crystal $CuGeO_3$ samples have been carried out in the diamond anvil cell using helium, argon, methanol/ethanol mixture, and other media[30]. A summary of the results is presented in Figure 8, deduced from the Raman spectra of the different phases. The Raman spectra of the three high pressure phases along with that of the normal phase are shown in Figure 9. The phase obtained under strictly

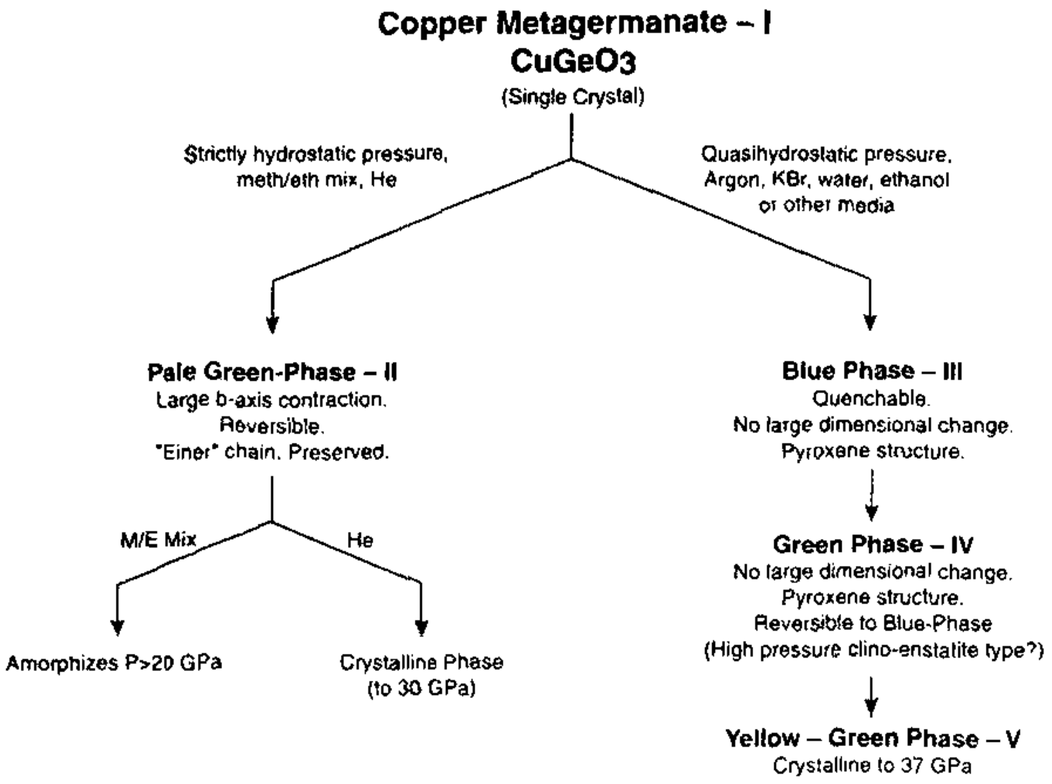

Figure 8. Sequence of phase transitions observed in copper metagermanate, under hydrostatic pressure and quasihydrostatic pressures, showing the totally different behaviour.

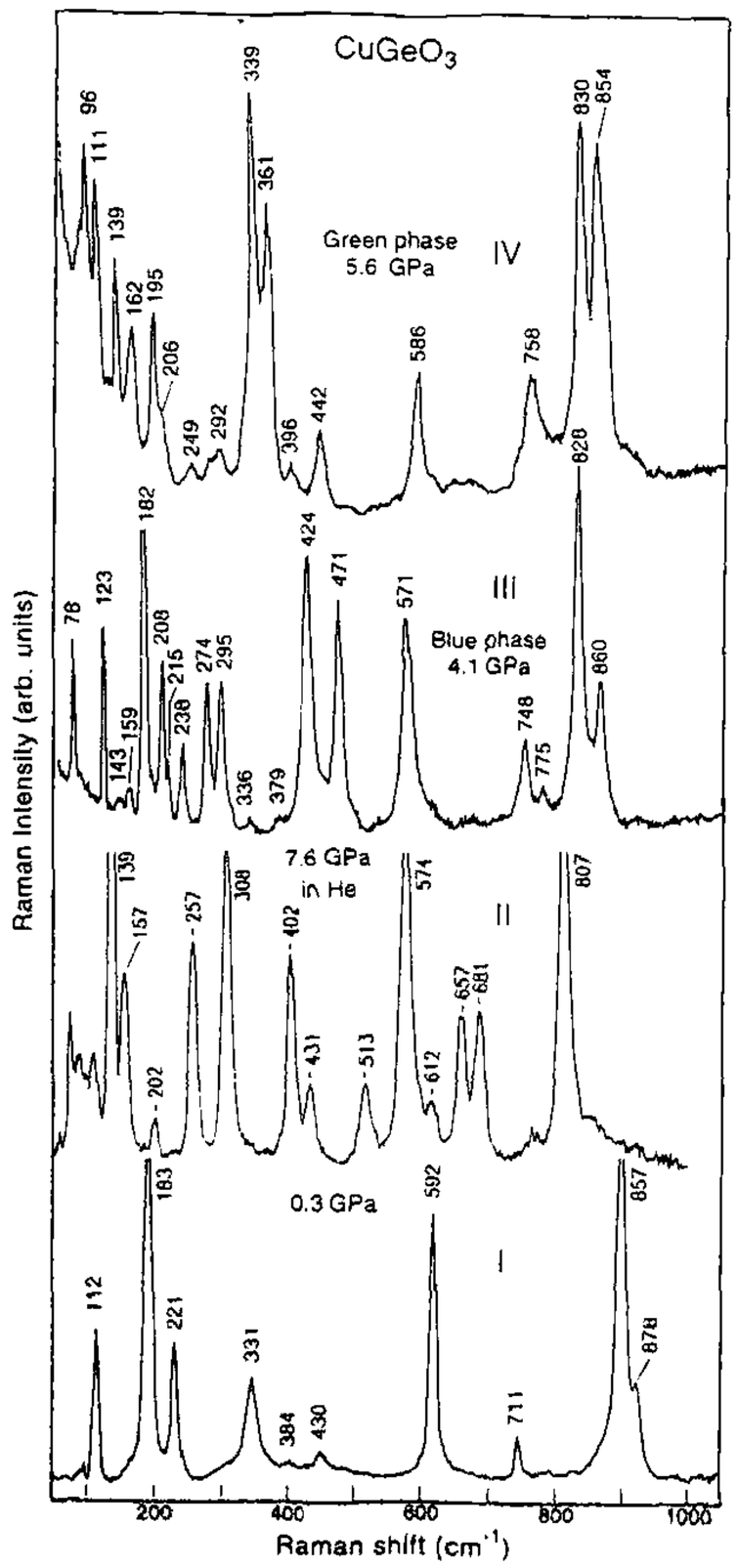

Figure 9. Raman spectra of the three high pressures phases, II, III and IV and the normal phase I of $CuGeO_3$.

hydrostatic conditions in the vicinity of 7 GPa has a Raman spectrum which suggests that the 'einer' chain character is preserved in the high pressure phase. Also, the crystal remains as a single crystal after the transition. The phase transition is reversible with a 2 GPa hysteresis. The elucidation of the structure of this high pressure phase awaits a high pressure single crystal X-ray diffraction study. This phase amorphizes when compressed in methanol/ethanol mixture, but with He as pressure medium no amorphization takes place and the system transforms to another crystalline phase.

Pressurization of the blue-phase in different pressure media leads to the same sequence as shown in Figure 8 and there is no amorphization up to 30 GPa, the highest pressure reached in our studies. The structures suggested for the blue-phase and the green-phase, namely the pyroxene type $MgSiO_3$ and its high pressure polymorph are supported by their Raman spectral features[31]. A high pressure X-ray diffraction study is needed to confirm the predictions. For the phases encountered at much higher pressures, the possibilities are ilmenite, garnet or perovskite type structures. Further studies, in particular high pressure X-ray diffraction studies, are expected to shed light on the nature of these phases.

Solid hydrogen at high pressure

The high pressure behaviour of solid hydrogen and deuterium has been of great interest[9] because of the possibility of their metallization under high pressure, predicted theoretically six decades ago. According to recent calculations, two types of metallic transitions, one in the molecular solid due to band overlap and the other due to the dissociation of the molecular to the atomic state in the solid, are expected[10].

In following, the high pressure behaviour of solid H_2 and D_2, Raman spectroscopy has played a crucial role and continues to be the most powerful probe. There is an interesting and untold story behind the use of Raman spectroscopy to probe hydrogen at high pressure. The publication of three apparently unrelated papers from different parts of the globe triggered the idea, namely (1) the first claim by Leonid Vereshchagin and his coworkers[32] that they got the metallic phase of hydrogen, in experiments with their diamond indentor device; (2) the observation that a Raman signal from solid Cl_2 could be obtained in the diamond cell, when Cl_2 was produced accidentally as a photo-decomposition product of CCl_4 in the cell by Adams and Sharma[33] and (3) the achievement of generating megabar pressures in the diamond cell by Mao and Bell[34]. Sharma *et al.*[35] first introduced Raman spectroscopy to study the high pressure behaviour of solid hydrogen and deuterium in the diamond cell, which turned out to be highly rewarding.

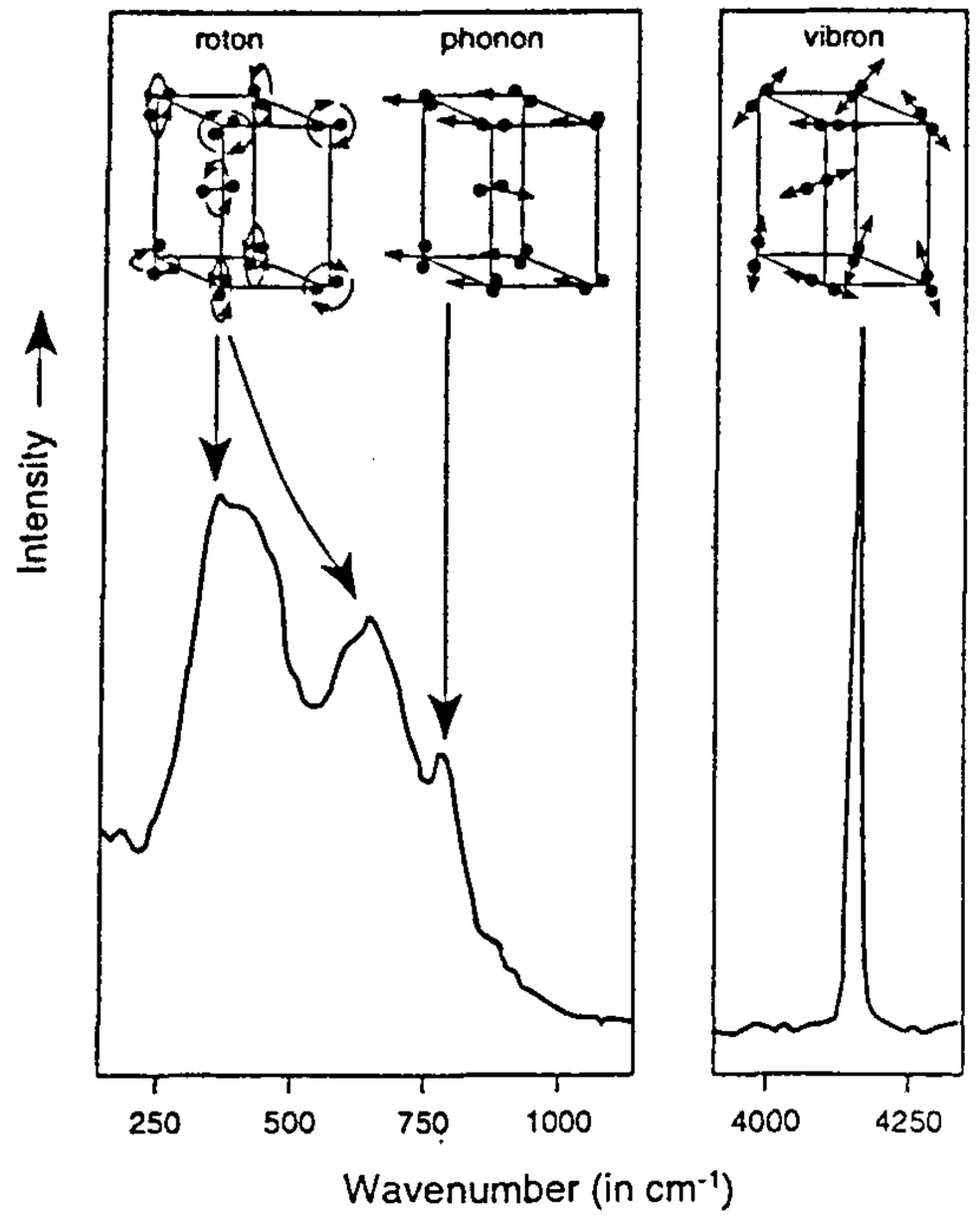

Figure 10. Vibrational modes in solid hydrogen showing the rotational (rotons), lattice vibrational (phonon) and the molecular stretching (vibron) modes, and below the observed Raman features corresponding to these at 96 GPa (ref. 6).

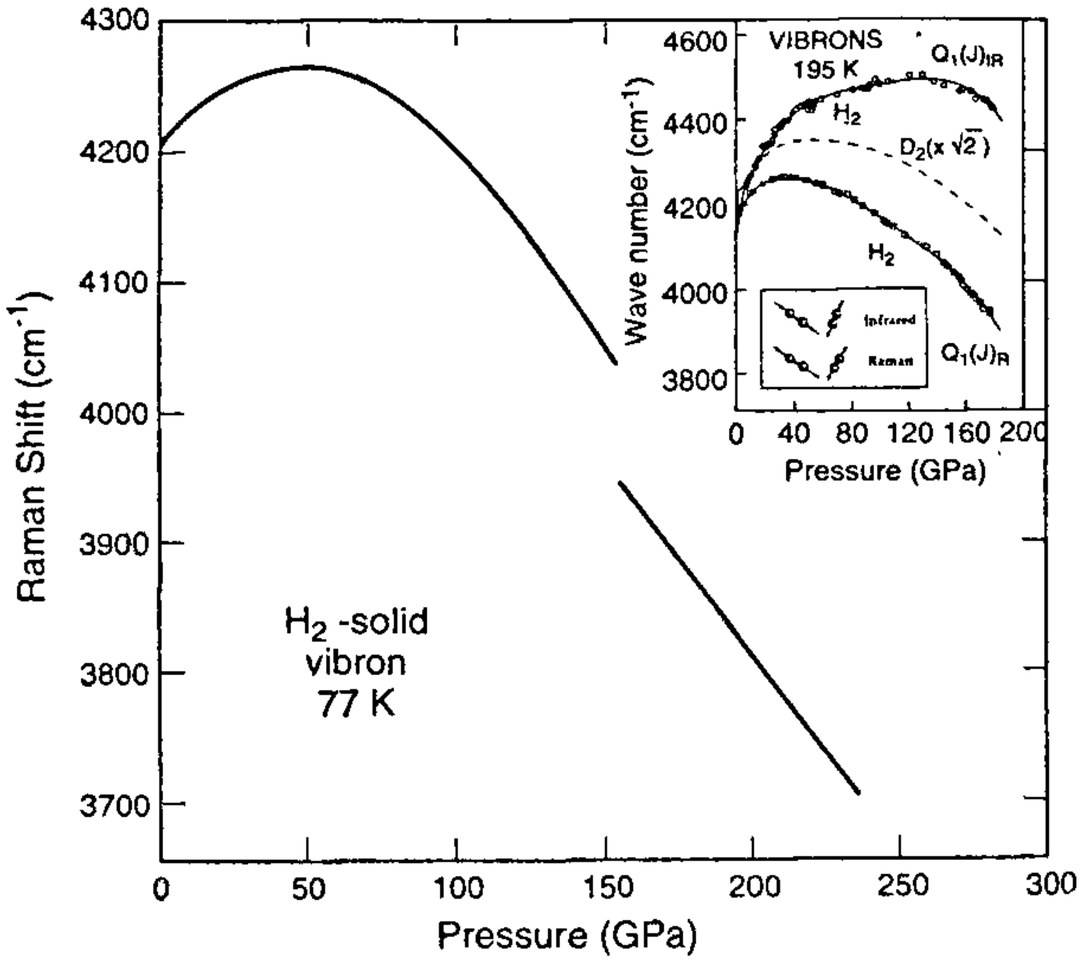

Figure 11. Pressure dependence of the vibron frequency of hydrogen at 77 K showing the unusual behaviour, the turnover and the abrupt drop of about 100 cm^{-1} near 150 GPa due to a transition from phase II (hcp) to phase III (A). The inset shows the pressure dependence of the vibron frequency in hydrogen and deuterium (dashed curve) at 295 K. Note the disappearance of the abrupt shift near 150 GPa. The top curve shows the IR active vibron which becomes very strong in phase III (A-phase).

There are three principal types of vibrational excitations in solid hydrogen (see Figure 10) and these are the stretching mode (vibron), the vibration of the lattice (phonon), and the rotations of the individual molecules (roton). The behaviour of these modes under pressure, namely, their frequencies and intensities, gives important clues as to what is happening to bonding, crystal structure and degree of orientational order. The stretching frequency of the molecule, called the vibron, is the strongest Raman peak observed with H_2 and D_2 and it has been followed up to about 2.5 megabar pressure in the diamond cell experiments. The turnover of the vibron frequency near 30 GPa (see Figure 11) is noteworthy and has given rise to much theoretical speculation[10] as to why it happens. Further, the break in the plot near 150 GPa is believed to be due to a first-order phase transition in solid hydrogen due to orientational ordering. A recent P–T diagram of hydrogen and deuterium arrived at using mostly the Raman data is shown in Figure 12 (ref. 36). The diagram is quite complex for simple materials like hydrogen and deuterium.

Hydrogen and its isotopes are quantum solids, for the reason that the zero-point energy and atomic motions have a considerable influence in the solid state. Their low temperature behaviour is marked by order–disorder transitions associated with the rotational state of the respective molecules[37]. With pressure, the effect of

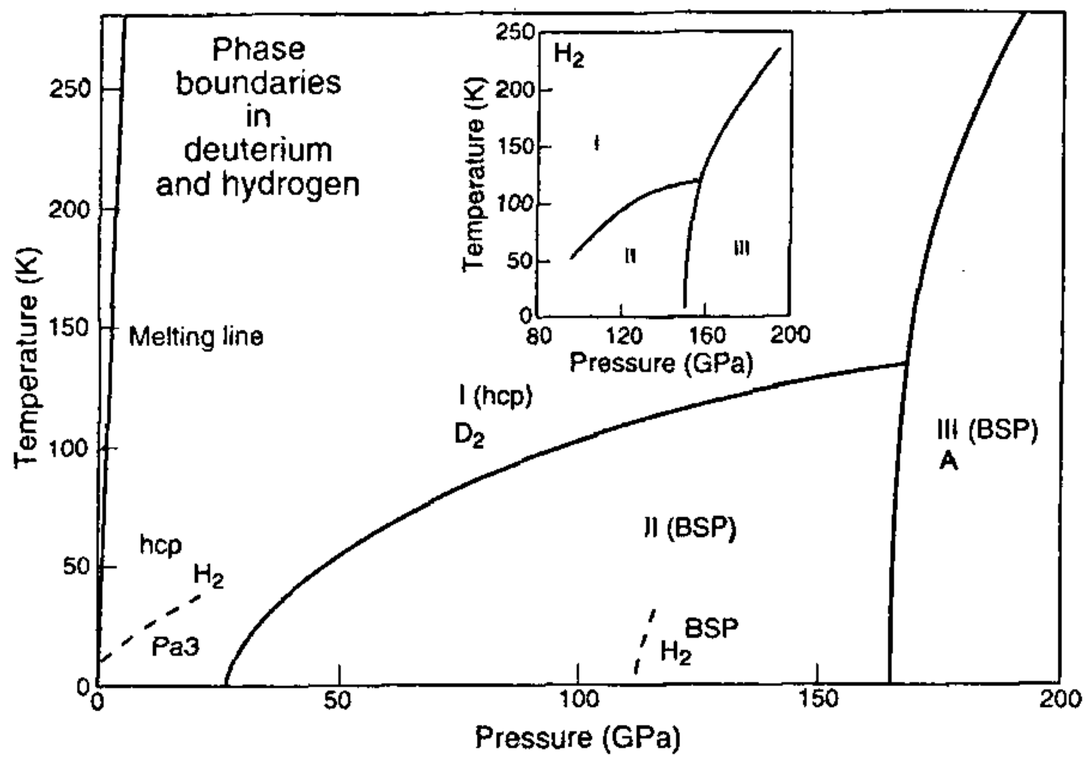

Figure 12. P–T diagram of solid H_2 and D_2 showing the different phases encountered; the boundaries were determined mainly from the Raman data. The inset shows the behaviour of solid hydrogen showing the triple point between phases I, II and III, first noted in solid D_2.

increasing intermolecular interactions overpowers the energy associated with the rotational states. The competition between the two leads to stabilization of the so-called broken symmetry phase (BSP). The structure of the BSP phases remains to be determined. The so-called A-phase first found by Hemley and Mao[38] in solid hydrogen near 150 GPa and 77 K has also been reported for D_2 solid[36]. According to Hemley and Mao, the discontinuity in the vibron frequency gradually disappears near 150 K and 150 GPa, which they interpreted as a critical point. However, this has been questioned[36] on the basis of symmetry arguments and the observation of strong infrared active vibron in the A-phase. Further, pressure–temperature excursions in D_2 in the vicinity of the transition of the A-phase suggest a triple point between the hcp-BSP-A-phase at 167 GPa and 130 K. Further detailed experiments show that a similar picture is true also for solid hydrogen, with the triple point at 160 GPa and 120 K (ref. 6). At higher temperature (~ 235°K and 182 GPa) the existence of a tricritical point has been proposed[39]. Transition to phase A (III) is believed to involve orientational ordering and broken symmetry. A clear picture will emerge when the structures of the high pressure phases of solid H_2 or D_2 are resolved.

Raman and IR spectroscopy, in combination with group theoretical analysis[36,40] and molecular dynamic calculations[41], have yielded some insight into the possible structure of the high pressure and low-temperature phases of hydrogen and deuterium. Accordingly, the most probable candidate structure for phase III (A-phase) seems to be *P2/m*. This would be consistent with the observed strong IR-active vibron and the Raman active vibron. Charge transfer and consequent development of a permanent dipole moment in an ordered orthorhombic structure (Pnma, $z = 4$) has been proposed for phase III, on the basis of a molecular dynamic simulation.

The stretching mode (vibron) is observed right up to the highest pressure studied, namely 230 GPa, which confirms that the D_2 and H_2 molecules are intact in solid hydrogen or deuterium compressed to 230 GPa. If dissociation to the atomic state were to occur, the vibron should disappear. The consensus at this time is that metallic hydrogen, either in the molecular state or by dissociation, has not yet been found in static compression of hydrogen and its isotope to 250 GPa. The topic is being hotly pursued at the Geophysical Laboratory of the Carnegie Institution of Washington, Harvard, and Cornell Universities.

Concluding remarks

The application of Raman spectroscopy in high pressure research has paid rich dividends, especially in studying materials which are transparent to visible radiation. It is a very convenient and fast *in situ* probe and can give insights into the microscopic aspects involved in phase transitions. In some areas like amorphization, it surpasses even the high pressure X-ray diffraction technique. Further, the use of single crystals in high pressure Raman studies with a hydrostatic pressure medium could be exploited to obtain information about the symmetry and together with powder X-ray diffraction data could lead to a complete understanding of the structure of the high pressure phase. Novel systems such as high T_c materials and fullerenes have been studied under high pressure using the Raman technique. But in general, Raman signals from systems opaque to laser radiation are much harder to get, and hence the use of Raman probe to study the high pressure behaviour of such systems is quite limited. The most interesting topic in condensed matter under high pressure at this time is the behaviour of solid hydrogen. In this field, Raman spectroscopy has been the mainstay and the tool *par excellence*. Without Raman and IR spectroscopy, the enormous progress that has been made in this field would not have been possible.

1. Jayaraman, A., in *Vibrational Spectra and Structure* (eds Bist, H. D., Durig, J. R. and Sullivan, J. F.), Elsevier Science Publishers, Amsterdam, 1989, vol. 17, pp. 93–114.
2. Sharma, S. K., Wang, Z. and van der Laan, S., *J. Raman Spectrosc.*, 1996, **27**, 739–746.
3. Jayaraman, A., *Rev. Mod. Phys.*, 1983, **55**, 65–108.
4. Jayaraman, A., Sharma, S. K., Wang, S. Y. and Cheong, S. W., *Phys. Rev.*, 1997, **B55**, 5694–5699.
5. Bell, P. M. and Mao, H. K., *Carnegie Institution of Washington Year Book*, 1979, **78**, 404–406; Hazen, R. M., Mao, H. K., Finger, L. W. and Bell, P. M., *Carnegie Institution of Washington Year Book*, 1980, **79**, 348–351.
6. Hemley, R. J., *Carnegie Institution of Washington Year Book*, 1994, **94**, 81–94; Loubeyre, P., LeToullec, R., Hausermann, D., Hanfland, M., Hemley, R. J., Mao, H. K. and Finger, L. W., *Nature*, 1996, **383**, 702–704.

7. Vohra, Y. K., Xia, H., Luo, H. and Ruoff, A. L., *Appl. Phys. Lett.*, 1990, **57**, 1007.
8. Mao, H. K. and Hemley, R. J., *Nature*, 1991, **351**, 721–724.
9. Vohra, Y. K., Proceedings of the International Conference on Condensed Matter at High Pressures, BARC, Bombay, India, Nov. 1996; Liu, J. and Vohra, Y. K., *Appl. Phys. Lett.*, 1996, **68**, 2049.
10. Mao, H. K. and Hemley, R. J., *Rev. Mod. Phys.*, 1994, **66**, 671–692.
11. Sugai, S., *J. Phys.*, 1985, **C18**, 799–808.
12. Hemley, R. J., Jephcoat, A. P., Mao, H. K., Ming, L. C. and Manghnani, M. H., *Nature*, 1988, **334**, 52.
13. Jayaraman, A., Wood, D. L. and Maines, R. G., *Phys. Rev.*, 1987, **B35**, 8316.
14. Sharma, S. M. and Sikka, S. K., *Prog. Mat. Sci.*, 1996, **40**, 1–77.
15. Sikka, S. K. and Sharma, S. M., *Curr. Sci.*, 1992, **63**, 317–320.
16. Jayaraman, A., Sharma, S. K., Wang, Z., Wang, S. Y., Ming, L. C. and Manghnani, M. H., *J. Phys. Chem. Solids*, 1993, **54**, 827–833.
17. Brixner, L. H., *Mat. Res. Bull.*, 1972, **7**, 879–892.
18. Jayaraman, A., Wang, S. Y. and Sharma, S. K., *Solid State Commun.*, 1995, **93**, 885–890.
19. Jayaraman, A., Wang, S. Y., Shieh, S. R., Sharma, S. K. and Ming, L. C., *J. Raman Spectrosc.*, 1995, **26**, 451–455.
20. Jayaraman, A., Wang, S. Y., Ming, L. C. and Cheong, S.-W., *Phys. Rev. Lett.*, 1995, **75**, 2356–2359.
21. Jayaraman, A., Wang, S. Y. and Sharma, S. K., *Phys. Rev.*, 1995, **B52**, 9896–9899.
22. Jayaraman, A., Wang, S. Y. and Sharma, S. K., *Curr. Sci.*, 1995, **69**, 44–48.
23. Jayaraman, A., Sharma, S. K. and Wang, S. Y., to be published.
24. Jayaraman, A., Wang, S. Y., Sharma, S. K. and Cheong, S.-W., *Curr. Sci.*, 1996, **70**, 232–234; Jayaraman, A., Sharma, S. K., Wang, S. Y., Shieh, S. R., Ming, L. C. and Cheong, S-W., *Pramana*, 1996, **47**, 151–161.
25. Jayaraman, A., Sharma, S. K., Wang, S. Y., Shieh, S. R., Ming, L. C. and Cheong, S.-W., *J. Raman Spectrosc.*, 1996, **27**, 485–490.
26. Hase, M., Terasaki, I. and Uchimokura, K., *Phys. Rev. Lett.*, 1993, **70**, 3651.
27. Völlenkie, H., Wittmann, A. and Nowotny, H., *Mon. Chem.*, 1967, **98**, 1352.
28. Liebau, F., *Structural Chemistry of Silicates*, Springer Verlag, Berlin, 1985; Lazarev, A. N., *Vibrational Spectra and Structure of Silicates*, Consultant Bureau, New York, 1972, p. 302.
29. Behruzi, M., Breuer, K. H. and Eysel, W., *Z. Kristallogr.*, 1986, **176**, 205–217; Breuer, K. H., Eysel, W. and Behruzi, M., *Z. Kristallogr.*, 1986, **176**, 219–232.
30. Jayaraman, A., Sharma, S. K., Wang, S. Y. and Cheong, S.-W., *Curr. Sci.*, 1996, **71**, 306–312; Goni, A. R., Zhou, T., Schwartz, V., Kramer, R. K. and Syassen, K., *Phys. Rev. Lett.*, 1996, **77**, 1079; Jayaraman, A., Sharma, S. K., Wang, S. Y. and Cheong, S.-W., *Phys. Rev.*, 1997, **B55**, 5694–5699.
31. Sharma, S. K., *Vib. Spectra Struct.*, 1989, **B17**, 513–560; Angel, R. J., Chopelas, A. and Ross, N. L., *Nature*, 1992, **358**, 322–324, Hugh-Jones, D. A., Woodland, A. B. and Angel, R. J., *Am. Mineral.*, 1994, **79**, 1032–1041.
32. Vereshchagin, L., *New Scientist*, 1976, **71**, 479; Yakovlev, Y., *New Scientist*, 1976, **71**, 478.
33. Adams, A. M. and Sharma, S. K., *J. Chem. Soc. Dalton Trans.*, 1976, 2424–2429.
34. Mao, H. K. and Bell, P. M., *Science*, 1976, **191**, 851–852.
35. Sharma, S. K., Mao, H. K. and Bell, P. M., *Phys. Rev. Lett.*, 1980, **44**, 886–888; Sharma, S. K., Mao, H. K. and Bell, P. M., *Carnegie Institution of Washington Year Book*, 1979, **78**, 645–649.
36. Cui, L., Chen, N. H. and Silvera, I. F., *Phys. Rev.*, 1995, **B51**, 14987–14997; Silvera, I. F., *J. Non Cryst. Solids*, 1996, **205–207**, 290–294.
37. Silvera, I. F., *Rev. Mod. Phys.*, 1980, **52**, 393–452.
38. Hemley, R. J. and Mao, H. K., *Phys. Rev. Lett.*, 1988, **61**, 857–860.
39. Goncharov, A. F., Mazim, I. I., Eggert, J. H., Hemley, R. J. and Mao, H. K., *Phys. Rev. Lett.*, 1995, **75**, 2514–2517.
40. Zallen, R., Martin, R. M. and Natoli, V., *Phys. Rev.*, 1994, **49**, 7032–7035.
41. Tse, J. S. and Klug, D., *Nature*, 1995, **378**, 595–597.

ACKNOWLEDGEMENT. This is SOEST contribution no. 4590 and H16P contribution no. 981.